Vol. 31 No. 133 *Journal of the Radio Research Laboratories* *July 1984*
Printed in Tokyo, Japan *pp. 111–132*

PRECISE ORBIT DETERMINATION OF A GEOSYNCHRONOUS SATELLITE BY ΔVLBI METHOD

By
Tadashi SHIOMI, Shin-Ichi KOZONO, Yoshinori ARIMOTO,
Seiji NAGAI, and Mitsuo ISOGAI

(Received on April 12, 1984)

ABSTRACT

An experiment was carried out to track a geosynchronous satellite by ΔVLBI method for 17 hours in the 4 GHz frequency band. A real time VLBI system with the baseline of 46 km was used, in which the system the observed data at the sub-station were transmitted to the main station via a microwave data link. Seven quasars were observed as reference sources. The geometrical delay was estimated with the accuracy of 0.3 nsec in the case of the satellite observations and 10 ~ 140 nsec in the case of the quasars. The finally obtained accuracy of the ΔVLBI observables was approximately 2 nsec (60 cm). The satellite orbit was determined with the accuracy of 100 m by using the ΔVLBI observables in addition to range and angle data which were obtained by a conventional radio tracking method. It was proved that ΔVLBI with appropriate baselines is a prospective method of precise tracking of a geosynchronous satellite for highly accurate orbit determination.

1. Introduction

One of the most established methods to track a geosynchronous satellite is the ranging at two or three earth stations. The accuracy of the range measurements has been improved up to approximately 1 m. In some cases, a ranging instrument is provided at a station A, and the other station B only retransmits the ranging signal which comes via the satellite from the station A. At the station A, the two-hop range from the stations A to B via the satellite is measured. In other case, the angles of the satellite are measured as well as the range at a station. In this case, high accuracy of the angle data is essentially required for the precise orbit determination. When the satellite transmits a beacon signal in a high frequency band (for example in 20 GHz band), an auto-tracking antenna with a narrow beam can provide angle data with the accuracy of 5×10^{-4} deg[1]. The orbit determination accuracy using those tracking data is approximately from a few hundreds to thousands of meters in the uncertainty of the satellite position. Some geosynchronous satellites (for example, the Tracking and Data Relay Satellite which has a function as a tracking station on the geosynchronous orbit), however, require higher accuracy in the orbit determination, that is to say, position uncertainty of within 100 m. Generally speaking, the requirement for higher accuracies of the orbit determination is being increased for satellites aiming at remote sensing, navigation, space VLBI, and so on.

On the other hand, a tracking method using VLBI has solved a problem which is an obstacle to the accurate orbit determination in the deep space navigation[2]. That is, it has been proved that VLBI measurement can provide angle data of a spacecraft in the deep space

with the accuracy of less than 10^{-6} deg and it takes less than one day of tracking span. On the contrary, a conventional radio tracking method of Doppler measurement supplies angle data with the accuracy of 10^{-5} deg, where the tracking span of several days or a few weeks is necessary.

It is expected that the VLBI method of tracking can be also applied to a geosynchronous satellite. In order to prove it, we carried out an experiment to track a geosynchronous satellite by differential VLBI (ΔVLBI) method. In the ΔVLBI, the difference between the observations of the satellite and a quasar which can be seen near the satellite produces highly accurate VLBI observables of the satellite under the assumption that the position of the quasar is known. As a method of tracking, VLBI has the following advantages: The earth stations need not have transmitting facilities, they only receive the radio waves emitted by the satellite and quasars. The VLBI can observe any kind of radio waves such as modulated communication signals, a beacon signal, or noise emitted from transponders of a satellite. The VLBI usually has very high sensitivity of signal detection and high accuracies of the observables. The ΔVLBI method provides absolutely calibrated observables by using quasars of which the positions are known precisely.

The Radio Research Laboratories (RRL) conducted an experiment of tracking the geosynchronous satellite ATS-1 by VLBI (not by ΔVLBI) with 2 MHz of receiving bandwidth and 125 km baseline spanned by Kashima and Yokosuka, both stations being located near Tokyo[3]. In the experiment, the differential ranges of the satellite at the two stations were obtained with the accuracy of approximately 4 m.

This paper describes an experiment which was carried out to track the geosynchronous satellite CS (Japan's Communications Satellite for Experimental Purposes) by ΔVLBI method with a length of 46 km, north-south baseline spanned by Kashima and Hiraiso stations of the RRL in June 1982. Seven quasars were used as reference natural radio sources. In the experiment, the differential ranges were obtained with the accuracy of 60 cm, and was proved the usefulness of the ΔVLBI method for highly accurate orbit determination of a geosynchronous satellite.

In Chapter 2 are described the principle of ΔVLBI method and the observational sensitivity of the VLBI with Kashima-Hiraiso baseline with respect to the orbit of the CS. Chapter 3 describes the system of the experiment and analyzes the errors due to system noises of the receiving systems and to other factors. Chapter 4 refers to the description on the method of the experiment and the schedule of the observations. Chapter 5 shows the methods of data reductions and the results. Chapter 6 is devoted to the analysis of the accuracy of orbit determination and of simulation studies to show the effectiveness of the ΔVLBI with higher accuracies and three longer baselines which are assumed in Japan. Finally, Chapter 7 gives the conclusion.

2. ΔVLBI method of tracking a geosynchronous satellite

2.1 Principle of ΔVLBI

ΔVLBI method can remove common errors to VLBI observables for two radio sources, one of which is a geosynchronous satellite and the other is a quasar. Using the ΔVLBI method, we obtain VLBI observables for the satellite with the same accuracy as that of quasar observations under ideal conditions, that is, with small separation angles between the satellite and each of quasars and with little variation in receiving system parameters between

the observations of the satellite and a quasar. The quasars of which the positions are known precisely are used. Fig. 1 shows a geometrical configuration of ΔVLBI method of tracking a geosynchronous satellite.

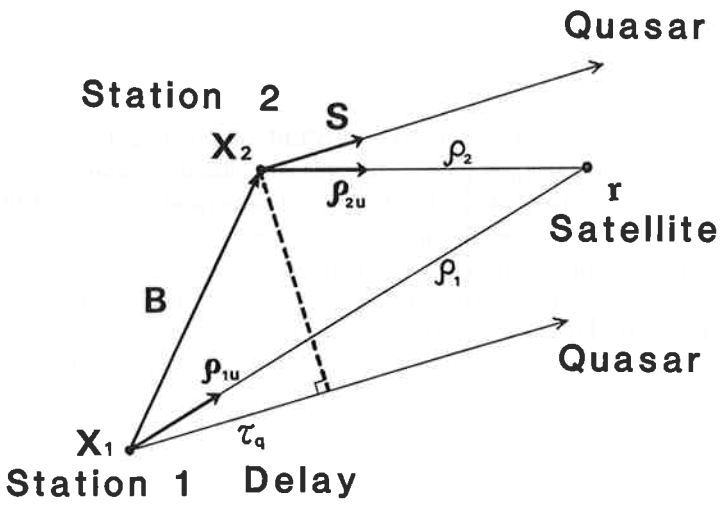

Fig. 1 Geometry of ΔVLBI observations

The delay observable for a quasar $\hat{\tau}_q$ is obtained by correlating the received signals. It is described as

$$\hat{\tau}_q = \tau_q + n_q \quad \cdots\cdots (1)$$

where τ_q is the geometrical delay and n_q means errors due to clock error, differential system delay between the two stations, differential delay due to the effects of the propagation media, and system noises. The n_q contains fixed or slowly varying term and inherently random term. The τ_q is given as

$$c\tau_q = \mathbf{S} \cdot \mathbf{B} \quad \cdots\cdots (2)$$

where

- c : velocity of light
- **S** : unit vector in the line-of-sight to the quasar
- **B** : baseline vector formed by the two stations which receive the same phase of the radio wave emitted by the quasar.

The delay observable for the geosynchronous satellite τ_S is given by

$$\hat{\tau}_S = \tau_S + n_S \quad \cdots\cdots (3)$$

$$\tau_S = \rho_1 - \rho_2 \quad \cdots\cdots (4)$$

where ρ_1 and ρ_2 correspond to the propagation times which are required for the same phase of the radio wave transmitted by the satellite to arrive at the two stations. The term n_s means a similar error to n_q in Eq. (1).

In the ΔVLBI method, we take the observable $\hat{\tau}_o$ which is the difference between $\hat{\tau}_q$ and $\hat{\tau}_s$, that is,

$$\hat{\tau}_o = \rho_1 - \rho_2 - \tau_q + n_s - n_q \quad \cdots\cdots (5)$$

When the above-mentioned ideal conditions for ΔVLBI are satisfied, the errors common to n_s and n_q are eliminated. The τ_q is given by Eq. (2) if we use the quasars of which the positions are known and the baseline vector is given. Consequently, the ΔVLBI observable provides the orbital information of the spacecraft in the form of $\tau_s = \rho_1 - \rho_2$ and it is not affected by the fixed errors, such as the differential system delays, clock error, the differential propagation delays at the two VLBI stations, and so on. The remaining random errors in the term of $n_s - n_q$ in Eq. (5) can be reduced by obtaining high signal-to-noise ratio in the VLBI observations. Section 3.2 gives some more explanations on this point.

The τ_s is described as

$$c\,\tau_s = \|\mathbf{r} - \mathbf{x}_1\| - \|\mathbf{r} - \mathbf{x}_2\| \quad \cdots\cdots (6)$$

where

$\mathbf{r}$: satellite position where the satellite transmitted the signal which is observed at the VLBI stations and correlated to give the delay

$\mathbf{x}_i$: position of station i where they receive the signal transmitted by the satellite.

The sensitivity of the observable $\hat{\tau}_o$ with respect to the small variation of the satellite position $\Delta\mathbf{r}$, to the error of the station location $\Delta\mathbf{x}_i$ and to the error of the quasar position $\Delta\mathbf{S}$ is given by the linearized form of Eq. (5) as

$$c\,\Delta\hat{\tau}_o = (\boldsymbol{\rho}_{1u} - \boldsymbol{\rho}_{2u}) \cdot \Delta\mathbf{r} - \boldsymbol{\rho}_{1u} \cdot \Delta\mathbf{x}_1 + \boldsymbol{\rho}_{2u} \cdot \Delta\mathbf{x}_2 - \mathbf{B} \cdot \Delta\mathbf{S} - \mathbf{S} \cdot (\Delta\mathbf{x}_2 - \Delta\mathbf{x}_1) \quad \cdots\cdots (7)$$

where Eqs. (2) and (6) are used, and

$\boldsymbol{\rho}_{iu}$: unit vector in the line-of-sight to the satellite at the station i.

The first term of Eq. (7) means that the ΔVLBI observable gives the information of motion of the satellite along the differential vector $(\boldsymbol{\rho}_{1u} - \boldsymbol{\rho}_{2u})$. The second and the third terms show the effects of the station location errors in the spacecraft VLBI observations.

2.2 Sensitivity of ΔVLBI with the Kashima-Hiraiso baseline

The sensitivity of ΔVLBI with the Kashima-Hiraiso baseline with respect to the CS orbit is evaluated by the first term of Eq. (7). The sensitivity vector $(\boldsymbol{\rho}_{1u} - \boldsymbol{\rho}_{2u})$ is given using the station location data in Table 1 (Chap. 3) as,

$$\boldsymbol{\rho}_{ku} - \boldsymbol{\rho}_{hu} = C_{kh}\,\boldsymbol{\rho}_{kh} \quad \cdots\cdots (8)$$

where

ρ_{ku} : unit vector in the line-of-sight to the CS at Kashima station

ρ_{hu} : unit vector in the line-of-sight to the CS at Hiraiso station

$C_{kh} = 9.36 \times 10^{-4}$

ρ_{kh} : unit vector

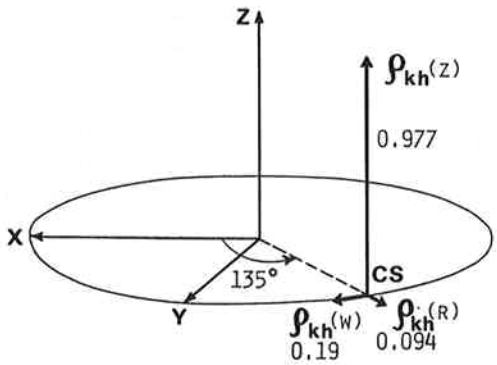

Fig. 2 Sensitivity of ΔVLBI with Kashima-Hiraiso baseline on the CS orbit

The unit vector ρ_{kh} is shown in Fig. 2. It is clear that the ΔVLBI observables with Kashima-Hiraiso baseline have the observational sensitivity for a position variation of the CS mainly in the north-south direction. The coefficient C_{kh} quantitatively represents the sensitivity. That is, let Δr_{kh} be a position variation of the CS in the north-south direction, then the corresponding variation in the ΔVLBI observable $\Delta\tau_{kh}$ is given as

$$c\,\Delta\tau_{kh} = C_{kh}\,\Delta r_{kh}, \quad \cdots\cdots (9)$$

Then it is possible to evaluate the sensitivity with respect to the CS position variation σ_r by

$$\sigma_r = c\,\sigma_{kh} / C_{kh} \quad \cdots\cdots (10)$$

where σ_{kh} is the accuracy of ΔVLBI observations. The σ_r is 1070 m for $c\,\sigma_{kh} = 1$ m, and it becomes 107 m when $c\,\sigma_{kh} = 10$ cm. Since the Kashima-Hiraiso baseline is short, the sensitivity is not so high. In order to determine the spacecraft position within the accuracy of 100 m, we should aim to obtain 10 cm accuracy of the ΔVLBI observables.

3. Observation accuracy

3.1 System of the experiment

Table 1 summarizes the ΔVLBI experiment system to track the CS. The VLBI system is called K-II VLBI[4] with two stations at Kashima and Hiraiso. The receiving frequency is in the 4 GHz frequency band. One of the characteristics of the K-II VLBI is that it is a real-time VLBI. The raw data received at Hiraiso station are digitized and formatted, then

Table 1 ΔVLBI tracking system for the CS

Stations	Kashima	Hiraiso
Longitude (East, deg)	140.662675	140.621737
Latitude (North, deg)	35.9542028	36.3679429
Geodetic height (m)	77.1346	71.6750
Reference ellipsoid	SAO-C7 : Re = 6378.142 km f = 1/298.255	
Baseline length (m)	46057.433	
VLBI System	Kashima	Hiraiso
Receiving antenna	26 m	10 m
Antenna gain	58.9 dB	48.9 dB
System noise	111 K	130 K
Receiving frequencies (MHz)	CH1: 4031, CH2: 4041, CH3: 4061, CH4: 4091, CH5: 4131	
Bandwidth	2 MHz/CH	
Sampling rate	4 Mbits/sec	
Frequency standard (stability 10 sec)	cesium (2.5×10^{-12})	rubidium ($< 1.6\times10^{-12}$)
Data transmission	Raw data of Hiraiso are transmitted to Kashima via a microwave data link	
Correlator	Real-time correlator, Lag 32 bits, Integration 10 msec	
Clock synchronization	using 1 sec pulses exchanged via the microwave link	
Clock calibration	using JJY with the accuracy ± 1 msec	
Geosynchronous satellite		
Satellite	Japan's Communications Satellite for Experimental Purposes (CS)	
Orbit	longitude 135 ± 0.1 deg E inclination 0.27 deg	
Satellite radio wave	noise emission of a transponder in the 4 GHz frequency band	
TT&C station	Kashima, tone ranging by 100 kHz tone, angle measurement by 19.45 GHz beacon	
Quasars	P0949+00, P1055+01, 3C273, 3C279, DW1335-12, NRAO530, 3C454.3	

transmitted to Kashima station via a microwave ground link. At Kashima station raw data of the two stations are correlated on the real-time base with the lag number of 32 bits (1 bit corresponds to 250 nsec), then the correlated data are integrated for 10 msec by using fringe stopping functions calculated through the predicted delay rate. The obtained complex correlation functions of every 10 msec are recorded on a digital magnetic tape with the time code, predicted delay and delay rate, bit-shifts number, and other necessary information. The post data reductions to get precise delay and delay rate are conducted later. The receiving bandwidth is 2 MHz per channel and the maximum number of receiving channels is five. Each channel is sequentially alternated every 100 msec. In our experiment, Channels 2 and 3 were used. The center frequencies of these channels are 4041 MHz and 4061 MHz, respectively.

The geosynchronous satellite CS has 2 transponders with the bandwidth of 200 MHz in the 4 GHz frequency band. We observed the noise emissions from one of the transponders. On the other hand, Kashima station has TT&C facilities for the CS. It is possible to perform

the ranging using 100 kHz tone signal via the TT&C link in the 4 GHz frequency band. The angles of the CS are measured by auto-tracking of the 19.45 GHz beacon signal by using a 13 m antenna. The ranging and angle measurements were made simultaneously with the ΔVLBI experiment.

3.2 Accuracies of VLBI observations

(1) SNR and estimation accuracies of the delay and the delay rate

The signal-to-noise ratio (SNR) in the VLBI observation is generally defined as[5]

$$SNR = L \cdot \sqrt{\frac{T_{a1}\, T_{a2}}{T_{s1}\, T_{a2} + T_{a1}\, T_{s2} + T_{s1}\, T_{s2}} \cdot 2BT} \quad \cdots\cdots (11)$$

where

T_{ai} : antenna temperature of the station i (i=1,2)

T_{si} : system noise of the station i (i=1,2)

B : receiving bandwidth

T : integration time

L : loss factor ($\fallingdotseq$ 0.4)

and T_{ai} is given as

$$T_{ai} = \frac{\lambda^2}{8\pi k} S\, G_i\, C_i \quad \cdots\cdots (12)$$

where

λ : wavelength of the receiving signal

k : Boltzmann's constant

S : flux density of a radio source

G_i : receiving antenna gain of the station i (i=1,2)

C_i : polarization matching coefficient at the station i ($i=1,2;\ 0 \leqslant C_i \leqslant 1$)

Equation (12) is applied to the case where one of the orthogonal polarizations is received. Suppose 4 GHz of the receiving frequency and assume $C_i = 1$, then T_{ai} is written in decibel form as

$$T_{ai}\ \mathrm{dB\ (K)} = -67.9 + G_i\ \mathrm{dB} + S\ \mathrm{dB\ (Jy)} \quad \cdots\cdots (13)$$

where 1 Jy = 10^{-26} W/m^2 · Hz.

In the quasar observations, since the relations $T_{a1}, T_{a2} \ll T_{s1}, T_{s2}$ are satisfied Eq. (11) becomes

$$SNR = L \cdot \sqrt{\frac{T_{a1}\, T_{a2}}{T_{s1}\, T_{s2}}\, 2BT} \quad \cdots\cdots (14)$$

The delay is obtained as the slope of the phase spectrum of the cross-spectral function which is the Fourier transform of the correlation function of the observed signals at the two VLBI stations. The variance of the estimated phase is inversely proportional to the square of SNR. So when the delay is obtained by the phases estimated in several observation channels, the standard deviation $\hat{\sigma}_\tau$ of the delay is given as

$$\hat{\sigma}_\tau = \frac{1}{\omega_{\text{eff}}\,\text{SNR}} \qquad \cdots\cdots (15)$$

$$\omega_{\text{eff}} = \sqrt{\sum_{i=1}^{K} (\omega_i - \bar{\omega})^2}\,,\ \bar{\omega} = \sum_{i=1}^{K} \omega_i / K$$

where

ω_{eff} : effective bandwidth

K : number of the observation channels

ω_i : observation frequency of the channel i

The SNR is evaluated for one channel. When the delay is estimated by the phases at several frequency points in only one channel, ω_i means the frequency of the sub-frequency band i in the channel, and K means the number of those bands. In this case, SNR is evaluated for each sub-frequency band.

The delay rate is obtained as the rate of the phase of the cross-spectral function. The standard deviation $\hat{\sigma}_{\dot{\tau}}$ is given as

$$\hat{\sigma}_{\dot{\tau}} = \frac{1}{\omega_o\, T_{\text{rms}}\, \text{SNR}} = \frac{1}{\omega_o\, T_{\text{eff}}\, \text{SNR}_t} \qquad \cdots\cdots (16)$$

$$\text{SNR}_t = \text{SNR} / \sqrt{M},\ T_{\text{eff}} = \sqrt{M}\, T_{\text{rms}} = \sqrt{\sum_{i=1}^{M} (t_i - \bar{t})^2}\,,\ \bar{t} = \sum_{i=1}^{M} t_i / M$$

where

ω_o : observation frequency

t_i : epoch time of the integration period i (i=1, 2,..., M)

SNR_t : signal-to-noise ratio evaluated for each integration period

(2) Accuracy of CS observations

The effective radiation power of the 4 GHz transponder noise (with no communication signals) of the CS is approximately 46.7 dBm. It gives the flux density of 31.0 dB (Jy) at the earth stations. Therefore, let S = 31.0 in Eq. (13) and consider that the receiving polarizations are matched to that of the CS radio wave at the VLBI stations, we obtain the antenna temperature T_c of the CS observation as

gains for those stations. That is, T_C (Kashima) = 25.0 dB (K) and T_C (Hiraiso) = 15.0 dB (K). The SNR of CS observations is given by Eq. (11) using these antenna temperatures and the system noise temperatures of the two stations, and the channel bandwidth B = 2 MHz, as

$$\text{SNR dB} = 25.2 + 1/2 \cdot \text{T dB (sec)} \quad \ldots\ldots\ldots\ldots\ldots\ldots\ldots\ldots\ldots\ldots\ldots\ldots (18)$$

where the loss factor L = 0.4 is used.

Suppose 10 sec of the integration T, then SNR is 30.2 dB. This SNR gives $\hat{\sigma}_\tau$ = 0.30 nsec (9.0 cm) by Eq. (15) with the effective bandwidth of 0.5 MHz (or $\omega_{\text{eff}} = 2\pi \times 0.5 \times 10^6$ rad/sec). Since the flux of the radio wave from the CS is strong, we obtain the desired accuracy of delay estimate with the integration for 10 sec from the viewpoint of system noise error.

(3) Accuracy of quasar observations

In the case of quasars, we should use Eq. (14). Using the antenna gains in Table 1, the antenna temperatures given in Eq. (13), and the bandwidth B = 2 MHz, SNR is given as

$$\text{SNR dB} = -5.8 + \text{S dB (Jy)} + 1/2 \cdot \text{T dB (sec)} \quad \ldots\ldots\ldots\ldots\ldots\ldots\ldots\ldots (18')$$

Since the correlation flux density of a quasar is mostly a few Janskies, we need much longer integration time than that of CS observations and observations in many frequency channels to improve the SNR.

As an example, we take the quasar 3C273 of which the correlation flux density is fairly strong, that is, in Eq. (18) S is approximately 13 dB (Jy). If we take 30 sec of integration time, SNR becomes 14.6 dB, which gives $\hat{\sigma}_\tau \doteq 11$ nsec (3.3 m) with the effective bandwidth of 0.5 MHz. In order to obtain higher accuracy of delay estimation, we should integrate the correlation function for longer time and obtain wider effective bandwidth.

Figure 3 shows the SNR and the accuracies of delay and delay rate estimates. Using Fig. 3, we obtain the SNR from the correlation flux density of a quasar and the integration time. Then, the accuracy of delay estimate is evaluated by the SNR and the effective bandwidth. The accuracy of delay rate estimate is evaluated by the SNR and the integration time. For example, an observation of 3C273 with the effective bandwidth of 20 MHz gives $\hat{\sigma}_\tau$ = 0.3 nsec with the integration for 30 sec.

(4) Errors in K-II VLBI

In the previous sections, the system noise errors in VLBI observations were studied. Here, other errors that affect the VLBI observables are evaluated. Those are position errors of quasars, station location errors (including geodetic coordinate errors, UT1 error and polar motion error), clock synchronization error, and correction errors of propagation media effects.

(i) Quasar position error

Since the baseline length of the K-II VLBI is 46 km, the quasar position error of 0.01 arc sec (2.8×10^{-6} deg) gives only 0.008 nsec (0.23 cm) of delay error. This error can be neglected in our experiment.

(ii) Station location error

Equation (7) shows that the difference of the components of the station location error vectors in the line-of-sights makes the error in delay observation. Denote the station location errors $\Delta\mathbf{x}_1$ and $\Delta\mathbf{x}_2$ for the stations 1 and 2, respectively. The angles between the line-of-

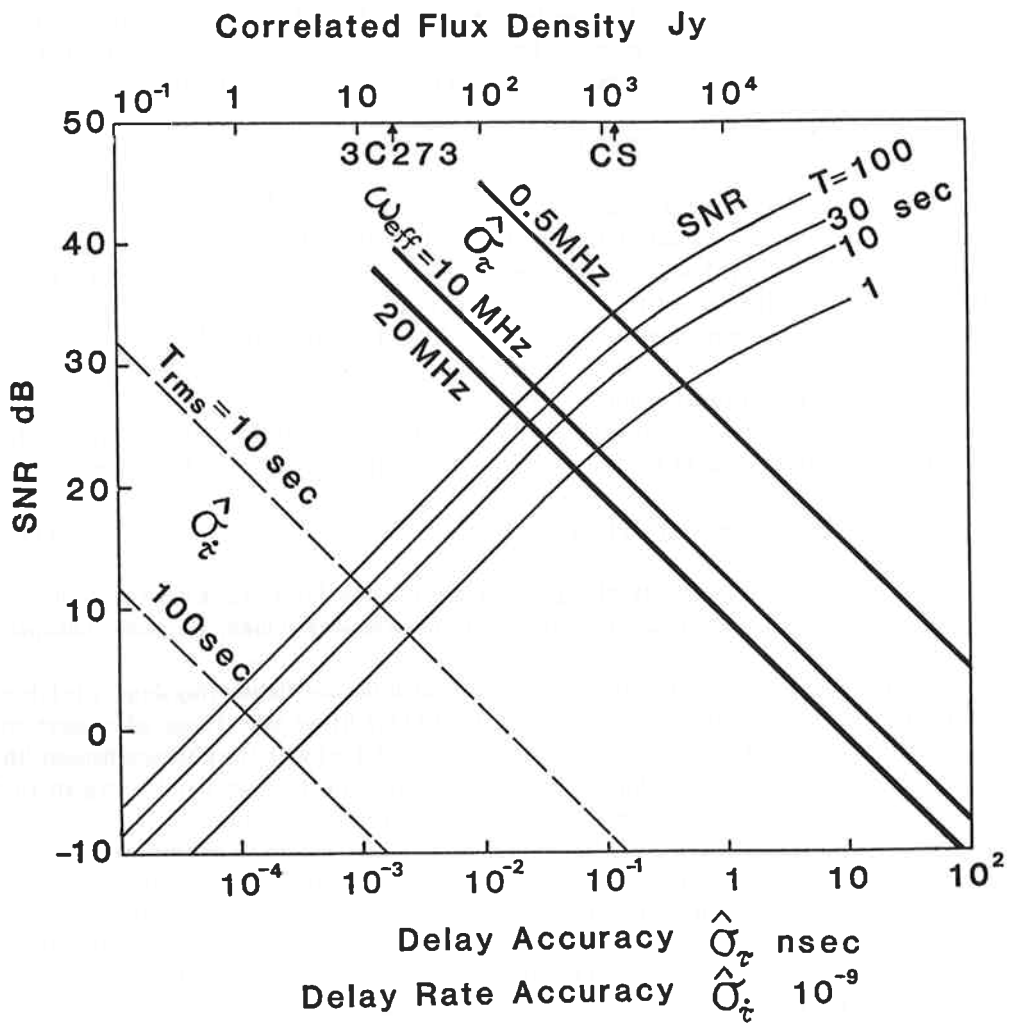

Fig. 3 Accuracy of ΔVLBI observations
Read SNR from given flux density of the radio source, then obtain the accuracies of the delay and the delay rate estimates.

sight of the CS and the station location error vectors $\Delta\mathbf{x}_1$, $\Delta\mathbf{x}_2$ are defined as θ_1 and θ_2, respectively, and the separation angles between the CS and a quasar at the two stations are $\Delta\theta_1$ and $\Delta\theta_2$, respectively (Fig. 4). Then, the delay observation error $\Delta\tau_S$ is written as

$$\begin{aligned} c\,\Delta\tau_S &= -\Delta x_1 \cos\theta_1 + \Delta x_2 \cos\theta_2 - \left\{ -\Delta x_1 \cos(\theta_1 + \Delta\theta_1) \right. \\ &\qquad \left. + \Delta x_2 \cos(\theta_2 + \Delta\theta_2) \right\} \\ &\fallingdotseq \Delta x_1 \sin\theta_1 \cdot \Delta\theta_1 - \Delta x_2 \sin\theta_2 \cdot \Delta\theta_2 \quad \cdots\cdots\cdots\cdots\cdots\cdots\cdots\cdots (19) \end{aligned}$$

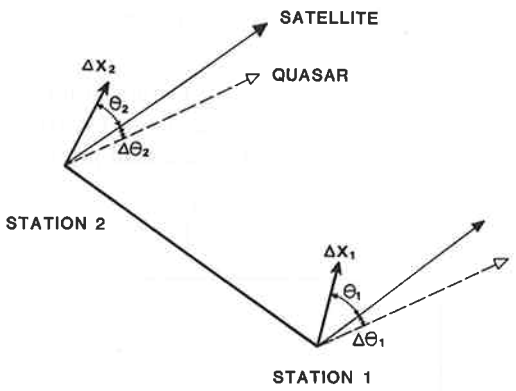

Fig. 4 Station location errors and their effects on ΔVLBI observables

where the separation angles $\Delta\theta_1$ and $\Delta\theta_2$ are small in ΔVLBI observations. In the short baseline VLBI, the components of $\Delta\mathbf{x}_1$ and $\Delta\mathbf{x}_2$, which are originated from the UT1 error and correction error of the polar motion, become very close and their contribution to $\Delta\tau_S$ is negligible since $\sin\theta_1 \cdot \Delta\theta_1$ and $\sin\theta_2 \cdot \Delta\theta_2$ also become close. The remaining components to be considered are the errors in geodetic data of the station coordinates. Let σ_{g1} and σ_{g2} be those errors for the stations 1 and 2, respectively. From Eq. (19) we obtain

$$c^2\,\Delta\tau_S^2 = \Delta\theta_1^2\,\sigma_{g1}^2 + \Delta\theta_2^2\,\sigma_{g2}^2 \quad \ldots\ldots\ldots\ldots\ldots\ldots\ldots\ldots\ldots\ldots\ldots\ldots\ldots\ldots (20)$$

Suppose $\Delta\theta_1 = \Delta\theta_2 = 10$ deg and $\sigma_{g1} = \sigma_{g2} = 20$ cm, then we get $\Delta\tau_S = 0.16$ nsec (4.9 cm).

(iii) Clock errors

The clock offset between the two stations is eliminated in ΔVLBI. But the variation of the offset between the observation times of a quasar and the satellite causes the error $\Delta\tau_T$ in the ΔVLBI delay observables as

$$\Delta\tau_T = \dot{\tau}_C \cdot \Delta t \quad \ldots\ldots\ldots\ldots\ldots\ldots\ldots\ldots\ldots\ldots\ldots\ldots\ldots\ldots\ldots\ldots\ldots\ldots\ldots\ldots (21)$$

where, $\dot{\tau}_C$ is the rate of the offset variation (or it is equivalent to the frequency difference of the atomic frequency standards at the two stations), Δt is the separation time between the observations of a quasar and the satellite. Let $\dot{\tau}_C = 0.1 \times 10^{-12}$ and $\Delta t = 10$ min, then we get $\Delta\tau_T = 0.06$ nsec (1.8 cm).

(iv) Effects of propagation media

The propagation media to be considered are the solar plasma, the magnetosphere of the earth, the ionosphere and the troposphere. The effect of the solar plasma is effective only in the quasar observations and it is small enough in our short baseline case. The effects of other media can also be eliminated by ΔVLBI within a few centimeters.

Concluding the above considerations, the errors in the ΔVLBI observables due to factors other than the system noises are about 0.2 ~ 0.3 nsec, which are within the desired accuracy of 10 cm.

4. Method of the experiment

4.1 Observation schedule

The tracking of the CS for 24 hours by ΔVLBI method using 11 quasars was planned, and the actual observations for 17 hours with 7 quasars were carried out. Fig. 5 shows the planned schedule and performed observations. Quasars with more than 1 Jy of correlation

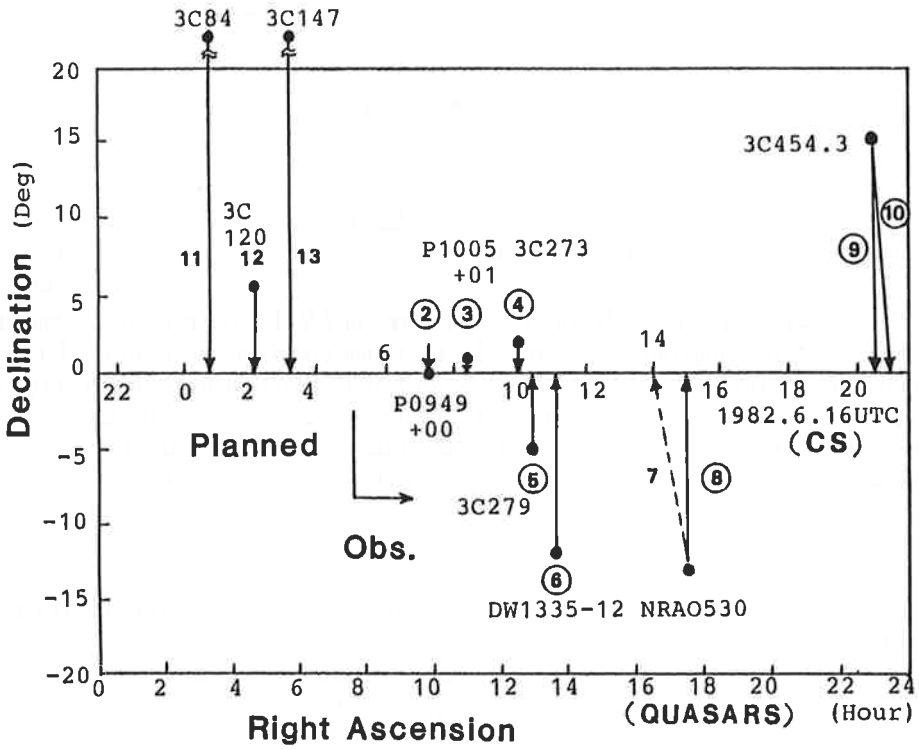

Fig. 5 ΔVLBI observation schedule
2 ~ 10 : observed by ΔVLBI method
7 : only the satellite was observed
11, 12, 13: planned only

flux density were used. Though some quasars were apart from the CS by more than 10 degrees, they were used because of their strong fluxes. Fig. 6 shows the viewing angles of quasars and the CS at the observation times at Kashima station.

Basically, one set of observations consisted of three consecutive ten-minutes of observations, that is, first a quasar was observed, then the CS, and again the quasar. It means that the CS observation is sandwiched between the quasar observations. This method makes easy to calibrate the CS observation by using the quasar observations. The first few minutes in the ten minutes pass are kept to point the receiving antennae to the radio source. The VLBI observation data were recorded for 45 seconds in the case of a quasar observation, and for 20 seconds in the case of the CS. The recordings were made during the last part of the ten-minutes pass, when the antennae completely tracked the radio source.

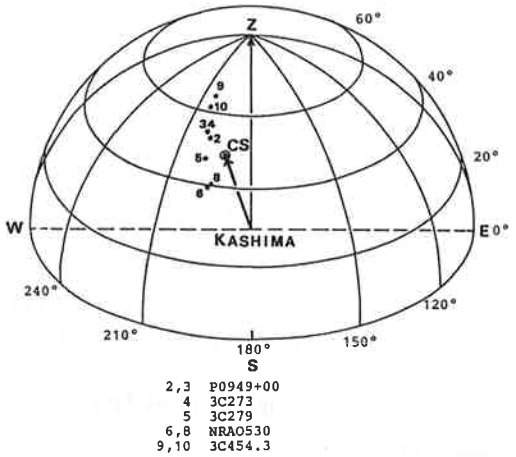

Fig. 6 Viewing angles of the radio sources at Kashima station
The figures show the observation numbers.

4.2 Control of the real-time correlator

The real-time correlator controls the bit-shifts of one of the signals received at the two stations and correlate them to produce cross-correlation function. Then it stops the fringe phase rotation using quantized fringe-stopping function and integrates the complex cross-correlation function for 10 msec. In the case of quasar observations, the fringe-stopping function of 10-levels of quantization was used. In the case of CS observations, no fringe stopping was applied and the correlation function was directly integrated for 10 msec, because the delay rate in a CS observation was less than $\pm 5 \times 10^{-11}$. Fig. 7 shows the predicted delay and delay rate for the CS observations.

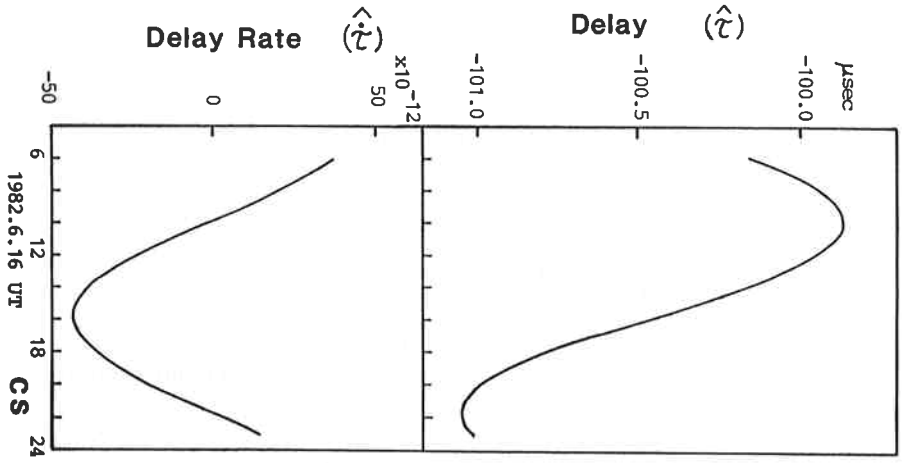

Fig. 7 Predicted delay and delay rate for CS observations

4.3 Clock calibration and synchronization

The cesium clock at Kashima station was calibrated by using Japanese broadcast standard time (JJY) to UTC within the error of ± 1 msec. Since the baseline is short and the difference between the longitude of the baseline vector and that of each object radio sources (CS and quasars) is small, the accuracy of ± 1 msec in the calibration is sufficient for our purpose. That is, in the K-II VLBI geometry, the ± 1 msec of clock errors of the stations to UTC, in other words, the corrresponding UT1 errors have little effect on the ΔVLBI observables.

The clock synchronization between the stations Kashima and Hiraiso was conducted within the error of 0.1 μsec by the method of transmitting pulses of 1 Hz via the microwave data link. This was sufficient to get a meaningful correlation in the real-time correlator.

5. Processing of ΔVLBI data

5.1 Method of delay estimation

The complex correlation function which is integrated for every 10 msec and recorded on a magnetic tape is written as,

$$R_{oxy}(t_i, \tau) = C_1 \sum_{t_i}^{\Delta t} \left\{ C_2 \cdot x(t+\tau)\, y(t-\tau_b)\, f(t) \right\} \quad \cdots\cdots\cdots\cdots\cdots (22)$$

where

$R_{oxy}(t_i, \tau)$: complex correlation function at the time t_i

C_1 : a coefficient multiplied to the complex correlation function when it is recorded on a magnetic tape

C_2 : coherence loss by infinite clipping $(2/\pi)$

$x(t)$: received signal at Kashima station

$y(t)$: received signal at Hiraiso station

τ_b : delay by bit-shifts (1 bit = 250 nsec)

$f(t)$: fringe-stopping function

$\sum_{t_i}^{\Delta t}$: integration for Δt (= 10 msec) from t_i

Denote the normalized complex correlation function $R_{xy}(\tau)$, it is described as

$$R_{xy}(\tau) = R_{oxy}(\tau)\, C_3 / (\Delta t\, C_1\, C_2) \quad \cdots\cdots\cdots\cdots\cdots\cdots\cdots\cdots (23)$$

where C_3 is the correction factor for quantization of the fringe-stopping function. The normalized cross-spectral function is obtained by integration of the Fourier transformed and phase-rotated cross-correlation function as

$$S_{xy}(\omega_k, t_i) = \frac{1}{\Delta t} \sum_{t_i}^{\Delta T} F\left[R_{xy}(t, \tau)\right] e^{-i\omega_k(\hat{\tau}-\tau_b)} \quad \cdots\cdots\cdots\cdots\cdots\cdots (24)$$

where

ω_k : video frequency, $\omega_k = 2\pi$ B k / 32,

B = 2 MHz, k = 0, 1, 2,..., 31

t_i : start time of the integration

$F[R_{xy}(\tau)]$: Fourier transform of $R_{xy}(\tau)$

$\hat{\tau}$: predicted delay

$\sum_{t_i}^{\Delta T}$: integration for ΔT from t_i

We used $\Delta T = 1$ sec. The phase-rotation in Eq. (24) is needed to correct the difference between the predicted delay and the delay by bit-shifts.

Let the delay residual $\Delta\tau$, the delay rate residual $\Delta\dot{\tau}$ and the delay acceleration residual $\Delta\ddot{\tau}$, then the estimates for them are given as those which make the following coherence function X_C maximum, that is,

$$(\Delta\tau, \Delta\dot{\tau}, \Delta\ddot{\tau}) = [\Delta\tau, \Delta\dot{\tau}, \Delta\ddot{\tau} | \max (X_C)] \quad \ldots\ldots\ldots\ldots\ldots\ldots\ldots\ldots\ldots\ldots (25)$$

$$X_C = \left| \frac{1}{T\omega_B} \sum^{T} \sum^{\omega_B} S_{xy}(\omega, t)\, e^{-i\omega\Delta t}\, e^{-i\omega_o (\Delta\dot{\tau} t + \frac{1}{2}\Delta\ddot{\tau} t^2)} \right| \quad \ldots\ldots\ldots\ldots\ldots\ldots (26)$$

where

T : integration time

ω_B : bandwidth

ω_o : observation frequency (CH2: 4041 MHz, CH3: 4061 MHz)

ω : video frequency (0 ~ 2 MHz)

$\sum^{T}$: integration with respect to the time span T

$\sum^{\omega_B}$: integration with respect to the video frequency span ω_B

In our data reductions, T is 30 sec for quasars and 20 sec for the CS. In fact, the effective integration time for each channel is the half of T, because the observations were conducted alternatively in Channels 2 and 3. In the case of CS observations, since the correlated flux density is strong enough, the above integration time is sufficient. It is better to integrate the quasar signals for longer time, but there exists practically a limit to the integration time due to the stabilities of the frequency standards at the two stations.

We processed all the data by the above mentioned method and obtained the delay and the delay rate estimates $\tau = \hat{\tau} + \Delta\tau$ and $\dot{\tau} = \hat{\dot{\tau}} + \Delta\dot{\tau}$ for the CS and quasars. Typical cross-spectral in the CS and quasar observations are shown in Fig. 8 and Fig. 9.

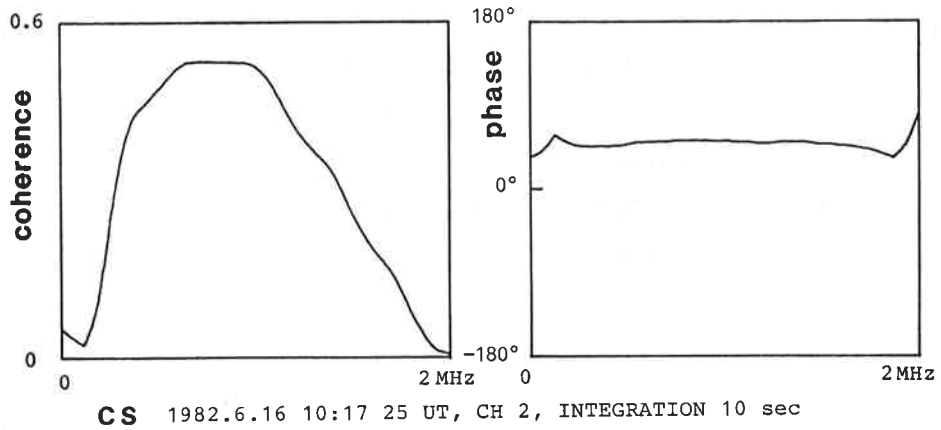

Fig. 8 Cross-spectral amplitude and phase of a CS observation

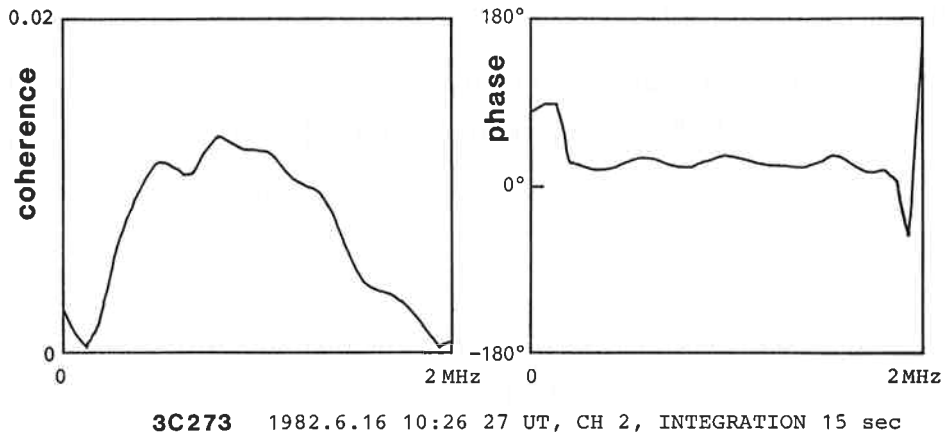

Fig. 9 Cross-spectral amplitude and phase of a quasar observation

5.2 Estimation of differential system delay

The delay estimates for the CS and quasars are shown in Fig. 10. Table 2 summarizes the coherences and accuracies of the delay estimates. As is expected by the evaluation in Sec. 3.2, the accuracy of the CS delay estimates is 0.3 nsec. In the case of quasars, it is in the range of 10 ~ 140 nsec.

Figure 10 shows the differences of the delay estimates between Channels 2 and 3, which are caused by the differences in the hardware performances of those channels. In the case of CS observations, they are pretty stable. The averages of them in the four time periods A, B, C and D in Fig. 10 are 152.46 nsec, 151.32 nsec, 151.56 nsec and 149.68 nsec, respectively.

We assume that those channel differences for CS can be also applied to the quasars. Then we convert Channel 3 delay estimates to those which are equivalent to Channel 2 delay estimates. They are shown in Fig. 11. We consider that the predicted delays for quasar